




Cite this: *Chem. Commun.*, 2025, 61, 15333

Received 28th July 2025,
Accepted 1st September 2025

DOI: 10.1039/d5cc04296h

rsc.li/chemcomm

Structure revision of meroterpenoid natural products enabled by biomimetic total synthesis

Jonathan H. George 

Meroterpenoids constitute a vast and structurally diverse family of natural products with mixed biosynthetic origins, found across nearly all forms of life on Earth. Despite their often intricate architectures, meroterpenoid biosynthesis follows a remarkably consistent and predictable chemical logic, driven largely by interactions between electron-rich aromatic rings and terpene-derived building blocks. However, the structural elucidation of these stereochemically complex molecules remains challenging, and misassignments are common. This review highlights the pivotal role of biomimetic total synthesis in enabling the structural reassignment of meroterpenoids, whilst also rationalising their biosynthetic origin, inspiring the design of novel cascade reactions, and even guiding the prediction and discovery of previously unknown natural products.

1. Introduction

For thousands of years, natural products – often in the form of unrefined plant extracts – have played a central role in treating human disease. Beginning in the mid-19th century, organic chemists started to approach the formidable task of unravelling the molecular structures of these complex and enigmatic compounds. Through chemical degradation, comparison with known substances, and ultimately total synthesis from simple

chemical feedstocks, these efforts laid the foundation for modern synthetic organic chemistry. The 20th century saw a transformative shift with the advent of physical analytical techniques such as ultraviolet and infrared spectroscopy, mass spectrometry, X-ray crystallography, and nuclear magnetic resonance (NMR) spectroscopy. These tools dramatically reduced the time and labour required for structural elucidation, diminishing the role of total synthesis as the definitive proof of structure. Nevertheless, the determination of complex natural product structures remains challenging, and incorrect structural assignments are still surprisingly common.¹

Among the physical methods available, NMR spectroscopy remains the most widely used for structure determination – and the most frequent source of error. Misinterpretations of 2D spectra (COSY, HSQC, HMBC, NOESY) can lead to mistakes in both atom connectivity and stereochemical configuration.² These challenges are exacerbated when working with limited sample quantities, poor signal-to-noise ratios, or compounds with low hydrogen-to-carbon ratios.³ In future, improving the reliability of NMR-based structure assignments may be achieved through broader sharing of raw spectral data,⁴ and through the automated comparison of chemical shifts across known compounds.⁵ More recently, the use of density functional theory (DFT) to predict NMR spectra has become a powerful and widely adopted tool for confirming or revising proposed structures,⁶ with dubious natural products often signposted using empirical rules or chemical intuition.⁷ Machine learning techniques are also beginning to enhance the accuracy of these predictions.⁸ While X-ray crystallography is generally more robust, it is limited by the need for high-quality crystals. However, innovations such as microcrystal electron diffraction (microED)⁹ and the use of crystalline sponges¹⁰ to host natural product analytes

School of Chemistry and Chemical Engineering, University of Southampton, Highfield, Southampton SO17 1BJ, UK.
E-mail: jonathan.george@southampton.ac.uk



Jonathan H. George

Jonathan George is an Associate Professor of Chemistry at the University of Southampton. He graduated with an MChem degree from the University of Oxford, and completed a PhD at University College London under the supervision of Prof. Karl Hale. After a postdoctoral position at the University of Oxford with Prof. Sir Jack Baldwin and Prof. Rob Adlington, he began his independent career in 2010 at the University of Adelaide. In

2024, he moved to his current position in Southampton, where his research continues to focus on the total synthesis, biosynthesis, isolation and structure elucidation of complex natural products.



are emerging as valuable tools for structure elucidation – particularly for minute or amorphous samples – enabling several recent structure revisions.

Despite the power of modern analytical and computational techniques, total synthesis continues to be an essential tool in resolving structural ambiguities.¹¹ Over the past fifteen years, my research group has investigated the synthesis, biosynthesis, and structural elucidation of complex meroterpenoids.¹² First defined by Cornforth in 1968,¹³ meroterpenoids are hybrid natural products derived from both terpene and non-terpene (often polyketide) biosynthetic origins.¹⁴ Today, the term typically refers to natural products combining aromatic polyketide and terpene motifs, frequently isolated from bacteria,¹⁵ fungi,¹⁶ plants,¹⁷ and marine organisms.¹⁸

In this personal account, several examples of meroterpenoid structure revisions enabled by total synthesis are highlighted. These biomimetic total syntheses all follow the biosynthetic logic inherent to the meroterpenoids, in which electron-rich aromatic polyketides are combined with terpene fragments in a predictable fashion, such as the geranylation of olivetolic acid to give cannabigerolic acid (Fig. 1(a)). Later steps in meroterpenoid biosynthesis often involve cycloadditions triggered by oxidation and transient dearomatization of phenolic rings, for example the intramolecular hetero-Diels–Alder reaction between a terpene side chain and the *ortho*-quinone methide (*o*-QM) derived from cannabigerolic acid forms the complex polycyclic ring system of tetrahydrocannabinol.¹⁹ The rapid generation of molecular complexity in meroterpenoid biosynthesis is further exemplified by the biogenetic origin of clusianone *via* the tetra-prenylation and permanent dearomatization of 2,4,6-trihydroxybenzophenone, followed by carbocation cyclization (Fig. 1(b)).²⁰ Both these biosynthetic pathways have inspired concise total syntheses that give insight into the structure and origin of meroterpenoid natural products.²¹

The biosynthetic logic that governs the interplay between aromatic polyketide and terpene motifs in meroterpenoids has enabled the anticipation of several structural revisions discussed in this account – often before they were experimentally confirmed through total synthesis. In some cases, however, our

total syntheses revealed inconsistencies in the originally proposed structures, prompting the identification of more plausible alternatives grounded in meroterpenoid biosynthetic reasoning. A common theme throughout the disparate synthetic strategies is the use of biomimetic cascade reactions set up by oxidative dearomatization of electron-rich aromatic rings.²² Many of the synthetic targets are stereochemically complex, but racemic, natural products, formed by highly predisposed reaction sequences.²³ Another unifying theme is the prediction and isolation of new natural products.²⁴ The first section of this account describes six cases in which structural reassignment involved major reorganization of atomic connectivity (Fig. 2), while the second section presents six examples of more nuanced structural corrections, each involving the reassignment of a single stereo-centre (Fig. 3).

2. Structure revisions involving an extensive reorganisation of the molecular structure

2.1 Hyperelodione D

Hyperelodione D is a cytotoxic meroterpenoid isolated from the *Hypericum elodeoides* flowering plant by Chen and co-workers in 2021.²⁵ The structure **1b** first proposed for hyperelodione D features a bowl-shaped, tetracyclic core adorned with geranyl substituents at C6a and C8 (Scheme 1(a)). The biosynthesis of **1b** was suggested to proceed *via* a cascade of Diels–Alder and Prins reactions between the symmetrical bis-geranylated quinone **18** and the monoterpene *E*- β -ocimene (**19**) (Scheme 1(c)).²⁶ This perfectly reasonable biosynthetic proposal was investigated in a biomimetic synthesis that commenced with bis-geranylation of commercially available 2,4,6-trihydroxybenzaldehyde (**16**) to give **17** in 33% yield.²⁷ Dakin oxidation of **17** using acidic H₂O₂, followed by FeCl₃-mediated oxidation of an intermediate hydroquinone, then furnished quinone **18** in good yield. However, the Lewis acid catalyzed Diels–Alder/Prins cascade reaction between **18** and commercially available *E*- β -ocimene (**19**) gave a tetracyclic product that exhibited very similar, but not identical, NMR data



Fig. 1 Representative examples of meroterpenoid logic in the biosynthesis of (a) tetrahydrocannabinol and (b) clusianone.





Fig. 2 Structure revisions involving an extensive re-organisation of the molecular structure.



Fig. 3 Structure revisions involving the correction of a single stereocentre.

to that reported for natural hyperelodione D. While the relative configuration and bond connectivity of the rigid 6–6–5–5 ring system of hyperelodione D could not be questioned, we realised that there were several alternative patterns of peripheral prenylation to consider as part of a structural reassignment. Close examination of 2D NMR spectra of natural hyperelodione D indicated that it contains only one geranyl group, located at C6a, with a prenyl substituent at C8 (Scheme 1(a)). We then proposed that the additional prenyl group required by the molecular formula could be “attached” to the C29 methyl substituent of

1b, thus implying a revised structure **1a** for hyperelodione D. Crucially, this revised structure could be formed from the known *Hypericum* natural products erectquione A (**13**)²⁸ and *E,E*- α -farnesene (**14**) via an intermolecular Diels–Alder reaction (*endo* T.S.) to give **15**, followed by a stereoselective, intramolecular Prins cyclization (Scheme 1(b)). Finally, this structural reassignment was validated by the biomimetic synthesis of structure **1a**. Synthesis of the unsymmetrical formylphloroglucinol derivative **20** followed by Dakin oxidation gave erectquione A (**13**), which underwent a Diels–Alder/Prins cascade





Scheme 1 (a) Suggested structure revision of hyperelodione D inspired by (b) biosynthetic hypothesis, revealed by (c) total synthesis of the originally proposed structure, and confirmed by (d) total synthesis of the reassigned structure.

reaction with synthetic *E,E*- α -farnesene (**14**)²⁹ to give hyperelodione D (**1a**), alongside a structural isomer (not shown) with the opposite pattern of prenylation/geranylation at C6a/C8 (Scheme 1(d)). Careful chromatographic separation of these isomers gave pure **1a**, which shared identical 1D and 2D NMR data with natural hyperelodione D, thus enabling a rather subtle structural reassignment that would have been difficult to achieve based on purely spectroscopic methods.

2.2 Rasumatranin D

Rasumatranin D is a complex meroterpenoid isolated from the Chinese liverwort *Radula sumatrana* in 2017 by Lou and co-workers.³⁰ However, we later suggested a revision of the initially assigned rasumatranin B structure **2b** both in terms of the position of the phenethyl side chain (from C7 to C5), and its relative

configuration at C11, to arrive at compound **2a** (Scheme 2(a)).³¹ The stereochemical reassignment was based on an observed coupling constant of 14 Hz between H3 and H11, and the absence of any NOE interaction between these hydrogen atoms, which suggested an unusual *trans* 5,5-ring junction in **2a**. The relative configuration of **2a** was also supported by comparison to related nyingchinoid³² and rhodonoid³³ meroterpenoids. The reassignment of the aromatic substitution pattern of rasumatranin D was based on our proposed biosynthesis of the natural product *via* an unusual [2+2+2] aerobic photocycloaddition of the known chromene meroterpenoid **21**³⁴ to give cyclic endoperoxide **22** (Scheme 2(b)). Intramolecular dearomatization of **22** to give *para*-epoxydienone **23** triggered by a thermodynamically favourable O–O cleavage, followed by an acid catalyzed C–C fragmentation and ring expansion that is driven by re-aromatization, would then



Scheme 2 (a) Suggested structure revision of rasumatranin D, inspired by (b) biosynthetic hypothesis, and confirmed by (c) total synthesis.



generate the revised rasumatranin D framework **2a**. This structure revision was proven through the bioinspired transformation of TBS-protected chromene meroterpenoid **24** into **2a** via a one-pot sequence of photoredox-catalyzed aerobic [2+2+2] photocycloaddition using a triarylpyrylium salt photocatalyst³⁵ to give **25**, TBAF-mediated dearomatization to give **23**, and a final acid catalyzed ring expansion (Scheme 2(c)). Spectroscopic data for the product **2a** was identical to that reported for natural rasumatranin D, thus confirming the structural reassignment.

2.3 Littoridials E and F

The meroterpenoids littoridials A–E were isolated from *Psidium littorale* (commonly known as strawberry guava) by Xu *et al.* in 2019.³⁶ While littoridials A–D (not shown) were all assigned plausible 6–6–9–4 ring systems that could be biosynthesised via hetero-Diels–Alder reactions between an *o*-quinone methide (*o*-QM)³⁷ and the reactive *trans* C4–C5 olefin of (–)-caryophyllene,³⁸ littorial E was proposed to possess a biosynthetically unlikely 7-membered ring in structure **3b** (Scheme 3(a)). Based partly on re-analysis of the isolation team's NMR data, we proposed that littorial E in fact contains a 6–6–9–4 tetracyclic ring system in revised structure **3a**, which could be derived from a hetero-Diels–Alder reaction between *o*-QM **26** and (–)-caryophyllene (**27**) (Scheme 3(b)).³⁹ This proposal was verified using a one-step, three-component biomimetic synthesis of the revised littorial E (**3a**), alongside its naturally occurring C9'-epimer littorial C (**30**), from commercially available diformylphloroglucinol (**28**), hexanal (**29**) and (–)-caryophyllene (**27**) (Scheme 3(c)). The mechanism of this biomimetic synthesis, which is inspired by Lee's classic total synthesis of guajadial and psidial A,⁴⁰ proceeds via condensation between **28** and **29** to generate *o*-QM **26** as a mixture of stereoisomers, followed by stereodivergent, intermolecular hetero-Diels–Alder reaction with **27** to give littoridials C and E. In addition to providing a sample of **3a** for further detailed spectroscopic analysis which matched the reported data for natural littorial E, its formation

via a biomimetic Diels–Alder-based strategy is strong evidence in favour of the proposed structural reassignment.

Another meroterpenoid – littorial F – was later isolated from strawberry guava and assigned structure **4b**, with an equally implausible 8-membered ring (Scheme 4(a)).⁴¹ Again, we suggested a reassignment of this natural product to a compound containing a more reasonable 6–6–9–4 ring system in **4a**, derived from an intermolecular hetero-Diels–Alder reaction between *ortho*-quinone methide **31** and (–)-caryophyllene (Scheme 4(b)). This structural reassignment was supported by a three-component synthesis of the revised littorial F (**4a**) in low yield, alongside the diastereomeric meroterpenoids littorial A (**33**) and littorial B (**34**), from a mixture of diformylphloroglucinol (**28**), butanal (**32**) and (–)-caryophyllene (**27**) (Scheme 4(c)).³⁹ It should be emphasised that the configurational assignment of the C4, C5 and C9' stereocentres across the littoridials is challenging due to their conformationally flexible 9-membered rings and overlapped signals in their ¹H NMR spectra. However, X-ray crystal structures for synthetic **30** and natural **33**, in addition to careful observation of NOESY correlations in synthetic **3a** and **4a**, eventually allowed full assignment of the littorial meroterpenoid family.

2.4 Cytosporolide A

Biosynthetic logic based on the intermolecular hetero-Diels–Alder reaction was also used in a structure revision of cytosporolide A, a meroterpenoid first isolated from a soil-dwelling *Cytospora* fungus collected from the Tibetan plateau.⁴² Originally proposed to have a highly strained 9-membered peroxy lactone ring in structure **5b**, we proposed a revised structure **5a** with a 6-membered aryl ether ring adjacent to a carboxylic acid instead of the unusual peroxy lactone system (Scheme 5(a)).⁴³ This was based on a biosynthetic pathway involving dehydration of the known fungal metabolite CJ-12,373 (**35**)⁴⁴ to give *ortho*-quinone methide **36**, followed by an intermolecular hetero-Diels–Alder with fuscoatrol A (**37**),⁴⁵ an oxidized caryophyllene



Scheme 3 (a) Suggested structure revision of littorial E, inspired by (b) biosynthetic hypothesis, and confirmed by (c) total synthesis.





Scheme 4 (a) Suggested structure revision of littordial F, inspired by (b) biosynthetic hypothesis, and confirmed by (c) total synthesis.

derivative that was co-isolated with cytosporolide A (Scheme 5(b)). We supported this proposed biosynthetic pathway through a biomimetic study involving condensation of **38** with triethyl orthoformate to give cyclic acetal **39** on route to the reactive *o*-QM **40**, which was trapped with caryophyllene (**27**) to give the simplified cytosporolide derivative **41** (Scheme 5(c)). While **41** shared some key NMR and IR data with natural cytosporolide A, a full structural reassignment was not complete until Takao's later total synthesis of the revised structure **5a** (Scheme 5(d)).⁴⁶ This was achieved using an intermolecular hetero-Diels-Alder reaction between a protected form of fuscocontrol A (**42**) and synthetic CJ-

12,373 (**34**), followed by deprotection of the intermediate **43** to give revised cytosporolide A (**5a**). This work also allowed the reassignment of cytosporolides B and C (not shown), which possess a very similar molecular architecture to cytosporolide A.

2.5 IsoBruceol

An unusual case of natural product structural clarification was inspired by our biomimetic total synthesis of bruceol (**6b**) – a meroterpenoid first isolated from the Western Australian plant *Philotheca brucei* by Jefferies and co-workers in 1963 (Scheme 6(a)).⁴⁷ While the structure of bruceol was proven by



Scheme 5 (a) Suggested structure revision of cytosporolide A, inspired by (b) biosynthetic hypothesis, supported by (c) biomimetic model studies, and confirmed by (d) Takao's total synthesis.



X-ray crystallographic studies, no detailed NMR data were originally reported by the isolation team at the University of Western Australia. About 30 years later, further analysis of natural products from *Philothea brucei* led Waterman and co-workers to publish NMR data for “bruceol”, which they thought they had re-isolated.⁴⁸ However, our biomimetic total synthesis of bruceol showed that Waterman had in fact isolated a similar but non-identical natural product, which we proposed could be “isobruceol” (**6a**).⁴⁹ This biosynthetically plausible meroterpenoid has the opposite orientation of the coumarin and terpene ring systems compared to bruceol. As shown in Scheme 6(b), the proposed biosynthesis of isobruceol occurs *via* epoxidation of chromene meroterpenoid **44** to give **45**, followed by epoxide ring-opening and intramolecular hetero-Diels–Alder reaction of the intermediate *ortho*-quinone methide **46** to give **6a**. The structural assignment of Waterman’s isobruceol was confirmed by its concise biomimetic synthesis from 5,7-dihydroxycoumarin (**47**) and citral (**48**),⁵⁰ which were condensed to give a separable mixture of two isomeric chromene meroterpenoids – protobruceol-I (**49**),⁵¹ which is the known biogenetic precursor of bruceol, and **50** (Scheme 11(c)). Isomerization of **50** *via* reversible ring-opening of the lactone ring on treatment with NaOMe gave a third chromene meroterpenoid isomer **44**, which was converted into isobruceol (**6a**) in low yield but high enantiopurity using a Jacobsen–Katsuki epoxidation⁵² with catalyst (*S,S*)-**51** to trigger the biomimetic, intramolecular hetero-Diels–Alder reaction. Synthetic **6a** perfectly agreed with the NMR data for Waterman’s natural product, and further X-ray analysis allowed us to confidently assign the isobruceol structure. For good measure, we also repeated the isolation of isobruceol from *Philothea brucei*, in addition to some biosynthetically related prenylated bruceol derivatives from *Philothea myoporoides*.⁵³

3. Structure revisions involving the reassignment of a single stereocentre

3.1 Hyperireflexolide B and enaimeones A and B

Hyperireflexolides A and B were isolated from *Hypericum reflexum*, a plant species in the St John’s wort family that is native to the Canary Islands, in 1993 by Pedro and co-workers.⁵⁴ Originally proposed to be highly oxidized terpenoid natural products, we realised that the unusual spirocyclic ring systems of the hyperireflexolides could instead arise *via* the rearrangement of a polycyclic polyprenylated acylphloroglucinol (PPAP) meroterpenoid, namely enaimeone A (**8a**), that is produced by the related species *Hypericum papuanum*.⁵⁵ While the structure of hyperireflexolide A (**61**) was determined by X-ray crystallography, our biosynthetic proposal required the structural reassignment of hyperireflexolide B at the spirocyclic C8-stereocentre, *i.e.* from structure **7b** to **7a** (Scheme 7(a)).⁵⁶ As shown in Scheme 7(b), our biosynthetic pathway begins with the fragmentation of enaimeone A (**8a**) *via* a retro-Dieckmann condensation to give a bicyclic lactone with fixed relative configuration at C5, C8 and C10. Aerobic oxidation at C12 to give a highly reactive 1,2,3-triketone **52** would set up an energetically favourable intramolecular carbonyl-ene reaction⁵⁷ with the pendant C8-prenyl group to give **53**. Finally, ring expansion of **53** *via* an unusual α -hydroxy- β -diketone rearrangement⁵⁸ would form the revised structure **7a** of hyperireflexolide B. Such a subtle structural reassignment was difficult to prove by re-evaluation of existing NMR data, so we embarked on a bioinspired total synthesis of both hyperireflexolides A and B (Scheme 7(c)). Geminal diprenylation of the simple acylphloroglucinol **54** with prenyl bromide under aqueous conditions gave **55** in 25% yield, alongside other di- and tri-prenylated by-products. Methylation of **55** at



Scheme 6 (a) Correction of the NMR data for bruceol and the discovery of isobruceol, inspired by (b) biosynthetic hypothesis, and confirmed by (c) total synthesis.





Scheme 7 (a) Suggested structure revision of hyperireflexolide B and enaimeones A and B, inspired by (b) biosynthetic hypothesis, and confirmed by (c) total synthesis.

C10 gave **56** in 41% yield, which contains all of the carbon atoms of the hyperireflexolide natural product targets. Oxidation of **56** with $\text{Mn}(\text{OAc})_3$ generates a β -diketo radical at C10, which can undergo a stereodivergent 5-*exo-trig* radical cyclization with one of the equivalent prenyl substituents, followed by trapping with O_2 and reduction with Zn, to give enaimeone A (**8a**) and enaimeone B (**8b**). Confusingly, enaimeones A and B had initially been misassigned at the C5 stereocentre due to ambiguous NMR analysis of the natural products, which both exist as mixtures of tautomers. However, we eventually assigned the correct structure **8a** to enaimeone A based on its facile conversion into the bicyclic lactone **57** via retro-Dieckmann fragmentation on heating in the presence of Hünig's base. Oxidation of **57** with Dess–Martin periodinane (DMP) then gave a separable diastereomeric mixture of spirocycles **53** and **58** via stereodivergent, intramolecular carbonyl-ene reactions of 1,2,3-triketone **52**. Finally, **53** and **58** underwent separate thermal α -hydroxy- β -diketone rearrangements to give hyperireflexolide A (via fragmentation of epoxide **59**) and the revised hyperireflexolide B (via fragmentation of epoxide **60**), with an X-ray crystal structure of **7a** confirming our structural reassignment.

3.2 Furoerioaustralasine

Furoerioaustralasine is an unusual quinoline meroterpenoid isolated by Waterman and co-workers from *Eriostemon banksii*, a flowering plant found in the Cape York Peninsula of Far North Queensland, Australia.⁵⁹ The stereochemically complex, pentacyclic structure **9b** was originally assigned to furoerioaustralasine based on 2D NMR studies (Scheme 8(a)). However, we suggested a reassignment of furoerioaustralasine to its C1'-

epimer **9a** due to its co-isolation with an epoxide-containing natural product, *cis*-erioaustralasine (**62**),⁶⁰ whose structure had been unambiguously defined by X-ray crystallographic studies. According to our biosynthetic hypothesis, hydrolysis of the *N*-acetoxymethyl group of **62** could trigger cyclization of 2-quinolone **63** via intramolecular $\text{S}_{\text{N}}2$ attack at the neighbouring epoxide (Scheme 8(b)). This $\text{S}_{\text{N}}2$ mechanism would invert the C2' stereocentre of **63** while retaining the C1' stereocentre, thus implying a structural reassignment of the product furoerioaustralasine to **9a**. Our suggested structure revision was confirmed by a simple biomimetic total synthesis (Scheme 8(c)).⁶¹ Condensation of 2,4-dihydroxyquinoline (**64**) with citral (**48**) gave the pyranoquinoline **65**,⁶² which was isomerised to tetracycle **66** under thermal conditions.⁶³ The major product, *cis*-fused tetracycle **66**, was separated from the minor *trans*-fused diastereomer (not shown) by selective crystallisation. Next, epoxidation of **66** with *m*-CPBA occurred stereoselectively on the less-hindered, convex face of the C1'-C2' alkene to give epoxide **63**,⁶⁴ which cyclised on exposure to TFA to give furoerioaustralasine. NMR analysis of our synthetic material matched Waterman's published data for the natural product, while single crystal X-ray crystallographic studies confirmed the revised structure **9a**.

3.3 Siphonodictyal B

Siphonodictyal B is a meroterpenoid derived from the marine sponge *Aka coralliphaga*, for which structure **10b** was proposed by Faulkner and Clardy in 1986 (Scheme 9(a)).⁶⁵ While studying the diverse range of bioactive meroterpenoids that were later isolated from *Aka coralliphaga*, we recognised that almost all exhibit the opposite configuration at the C8 stereocentre compared to





Scheme 8 (a) Suggested structure revision of furoerioaustralasine, inspired by (b) biosynthetic hypothesis, and confirmed by (c) total synthesis.

siphonodictyal B. For example, liphagal (**67**)⁶⁶ and corallidictyals A–D (**68–71**)⁶⁷ all feature a stereocentre at C8 in the *R* configuration, while in the proposed structure of siphonodictyal B (**10b**) the corresponding C8 stereocentre is *S* (Scheme 9(b)). Given that these meroterpenoids would probably share a common biosynthetic pathway in the marine sponge, we proposed that siphonodictyal B be revised to **10a**, and that this structure is the direct biogenetic precursor of liphagal and corallidictyals A–D. This hypothesis was proven *via* semi-synthesis of **10a** from (+)-sclareolide (**72**),⁶⁸ which showed identical spectroscopic properties to natural siphonodictyal B (Scheme 9(c)). The close relationship between the *Aka coralliphaga* meroterpenoids was then underlined by the conversion of the revised structure of siphonodictyal B (**10a**) into liphagal (**67**) *via* a sequence of epoxidation, pinacol rearrangement and benzofuran formation,⁶⁹ into corallidictyals A and B (**68** and **69**) by aerobic oxidation, and into corallidictyals C and D (**70** and **71**) by acid catalyzed cyclization.⁷⁰ This highly divergent synthetic strategy highlights how pattern recognition within a family of natural products isolated from a common biological source can identify possible structural misassignments. Finally, our work suggests that some

sulfated derivatives of siphonodictyal B that were subsequently discovered in *Aka coralliphaga* marine sponges – namely siphonodictyals B1, B2, and B3 – should also be revised at the C8 stereocentre.⁷¹

3.4 Anthopogochromane

Anthopogochromane is a merosequiterpenoid isolated from *Rhododendron anthopogonoides* by Iwata *et al.* in 2010.⁷² The unusual 6–6–6–4 ring system of the originally proposed structure **11b** was derived from 2D NMR studies. However, our synthetic studies on the structurally similar rubiginosin meroterpenoids⁷³ led us to propose a structural reassignment of anthopogochromane to its C13 epimer, **11a** (Scheme 10(a)).⁷⁴ The biosynthesis of anthopogochromane could occur *via* oxidation of the terpene side chain of daurichromenic acid (**73**) to give enone **74**, with the C12–C13 alkene adopting a more stable *E* configuration (Scheme 10(b)). Stereoselective, intramolecular [2+2] cycloaddition of **74** with retention of the alkene geometry would then give the revised anthopogochromane structure **11a**, with the C13 ketone substituent adopting a less sterically



Scheme 9 (a) Suggested structure revision of siphonodictyal B, inspired by (b) biosynthetic connections to related marine meroterpenoids, and confirmed by (c) total synthesis.





Scheme 10 (a) Suggested structure revision of anthopogochromane, inspired by (b) biosynthetic hypothesis, and supported by (c) the total synthesis of rubiginosin G.

demanding *exo* orientation relative to the bowl-shaped 6–6–6–4 ring system. The structure revision of anthopogochromane was supported by the biomimetic total synthesis of rubiginosin G (79), which has the same structure as anthopogochromane minus the carboxylic acid group at C6 (Scheme 10(c)). Condensation of orcinol (75) with unsaturated aldehyde 76 gave a known chromene meroterpenoid, rubiginosin D (77). Intramolecular [2+2] cycloaddition of 77 catalyzed by FeCl₃ then gave rubiginosin A (78) as a single diastereomer,⁷⁵ which was hydrogenated to give rubiginosin G (79). Comparison of NMR data for synthetic 79 with that reported for anthopogochromane showed near identical and highly diagnostic chemical shifts, coupling constants and NOE interactions for H3, H4 and H13 around the key cyclobutane ring, strongly indicating that the structure of anthopogochromane should be revised to 11a.

3.5 Atrachinenin C

Atrachinenin C is a complex meroterpenoid recently isolated from *Atractylodes chinensis*, a traditional Chinese medicinal plant, by Chen *et al.* in 2022.⁷⁶ Shortly afterwards, we revised the originally proposed atrachinenin C structure 12b to its C12-epimer 12a (Scheme 11(a)) based on some unexpected results of our biomimetic synthetic studies.⁷⁷ As outlined in Scheme 11(b), the revised biosynthetic pathway to atrachinenin C (12a) begins with an *endo*-selective intramolecular Diels–Alder reaction between *E*-β-ocimene (19) and the known quinone meroterpenoid 80⁷⁸ to give 81, followed by stereoselective epoxidation of the prenyl side chain and 5-*exo-tet* cyclization of the resultant epoxide 82. This revised biogenetic pathway and structural reassignment of atrachinenin C stemmed from the synthesis of two simplified analogues, the C12 epimers 87 and 90, with only compound 90 bearing close resemblance to the natural product (Scheme 11(c)). The model study began with an on-water catalyzed, intermolecular Diels–Alder reaction⁷⁹ between 2,6-dimethylquinone (83) and *E*-β-ocimene (19) to give the *endo* adduct 84. Photoredox-catalyzed, intramolecular [2+2] cycloaddition of the enol 85 derived from

enedione 84 then gave cyclobutanol 86,⁸⁰ which underwent oxidative fragmentation⁸¹ with PhI(OAc)₂ to give an interconverting mixture of the atrachinenin C analogue 87 and its ring-closed cyclic hemiacetal form 88 (1.3:1 ratio in CDCl₃). This contrasts with natural atrachinenin C, which exists only in a ring-opened keto form. NMR data for 87 also differs significantly from that reported for natural atrachinenin C, particularly ¹H and ¹³C signals around the key C12 stereocentre. We therefore synthesised the model C12 epimer 90 *via* base catalyzed 5-*exo-tet* ring-opening of epoxide 89 (used as a mixture of diastereomers), which resulted in a complex mixture of 90, 87 and 88 (2.1:1.6:1 ratio in CDCl₃). Comparison of the NMR data for carefully purified 90 showed excellent agreement with that reported for atrachinenin C, thus supporting its reassignment to structure 12a.

4. Conclusion

The simple, efficient, and logical biosynthetic pathways leading to meroterpenoids have inspired numerous concise total syntheses of these complex natural products by our research group. In some cases, the motivation for synthesis stemmed directly from the need to resolve structural ambiguity; in others, structural reassignment emerged as an unexpected – though not unwelcome – outcome during the course of the work. In both scenarios, we have demonstrated that a holistic approach to meroterpenoid chemistry – encompassing total synthesis, biosynthetic analysis, isolation studies, spectroscopic techniques, and computational methods – can yield powerful insights into the structural elucidation of intricate natural products. This dynamic field has also seen notable contributions from other groups, with recent structural reassignments of meroterpenoids based on total synthesis,⁸² DFT calculations,⁸³ and NMR methods.⁸⁴ And while some have recently questioned the role of total synthesis in structure determination,⁸⁵ we maintain that it remains the gold standard for attaining a deep and unambiguous understanding of the structure and character of a natural product.





Scheme 11 (a) Suggested structure revision of atrachinenin C, inspired by (b) biosynthetic hypothesis, and supported by (c) biomimetic model studies.

Conflicts of interest

We declare no conflict of interest.

Data availability

No primary research results have been included and no new data were generated or analysed as part of this feature article.

Acknowledgements

gratefully acknowledge the support of the Australian Research Council (DE130100689, FT170100437, DP160103393, DP200102964) for funding this research. I also extend my warmest thanks to the former members of my research group at the University of Adelaide, whose enthusiasm, dedication, and good humour made these projects so richly enjoyable during my time in Australia.

References

- For general reviews of natural product structure revision, see: (a) B. K. Chhetri, S. Lavoie, A. M. Sweeney-Jones and J. Kubanek, *Nat. Prod. Rep.*, 2018, **35**, 514; (b) S.-M. Shen, G. Appendino and Y.-W. Guo, *Nat. Prod. Rep.*, 2022, **39**, 1803.
- D. C. Burns and W. F. Reynolds, *Magn. Reson. Chem.*, 2021, **59**, 500.
- P. J. Sidebottom, *Magn. Reson. Chem.*, 2021, **59**, 752.
- J. B. McAlpine, S.-N. Chen, A. Kutateladze, J. B. MacMillan, G. Appendino, A. Barison, M. A. Beniddir, M. W. Biavatti, S. Bluml, A. Boufridi, M. S. Butler, R. J. Capon, Y. H. Choi, D. Coppage, P. Crews, M. T. Crimmins, M. Csete, P. Dewapriya, J. M. Egan, M. J. Garson, G. Genta-Jouve, W. H. Gerwick, H. Gross, M. K. Harper, P. Hermanto, J. M. Hook, L. Hunter, D. Jeannerat, N.-Y. Ji, T. A. Johnson, D. G. I. Kingston, H. Koshino, H.-W. Lee, G. Lewin, J. Li, R. G. Linington, M. Liu, K. L. McPhail, T. F. Molinski, B. S. Moore, J.-W. Nam, R. P. Neupane, M. Niemitz, J.-M. Nuzillard, N. H. Oberlies, F. M. M. Ocampos, G. Pan, R. J. Quinn, D. Sai Reddy, J.-H. Renault, J. Rivera-Chávez, W. Robien, C. M. Saunders, T. J. Schmidt, C. Seger, B. Shen, C. Steinbeck, H. Stuppner, S. Sturm, O. Tagliatela-Scafati, D. J. Tantillo, R. Verpoorte, B.-G. Wang, C. M. Williams, P. G. Williams, J. Wist, J.-M. Yue, C. Zhang, Z. Xu, C. Simmler, D. C. Lankin, J. Bisson and G. F. Pauli, *Nat. Prod. Rep.*, 2019, **36**, 35.
- (a) E. Guerrero De Leon, H. Sanchez-Martinez, J. A. Moran-Pinzon, E. del Olmo Fernandez and J. L. Lopez-Perez, *J. Nat. Prod.*, 2023, **86**, 897; (b) H. Sanchez-Martinez, J. A. Moran-Pinzon, E. del Olmo Fernandez, D. Lopez Eguiluz, J. F. Asderias Vistue, J. L. Lopez-Perez and E. Guerrero De Leon, *J. Nat. Prod.*, 2023, **86**, 2294.
- For recent reviews of the role of computational calculations in natural product structure assignment, see: (a) D. C. Burns, E. P. Mazzola and W. F. Reynolds, *Nat. Prod. Rep.*, 2019, **36**, 919; (b) M. O. Marcarino, M. M. Zanardi, S. Cicetti and A. M. Sarotti, *Acc. Chem. Res.*, 2020, **53**, 1922; (c) M. Elyashberg and D. Argyropoulos, *Magn. Reson. Chem.*, 2021, **59**, 669; (d) F. L. P. Costa, A. C. F. de Albuquerque, R. G. Fiorot, L. M. Liao, L. H. Martorano, G. V. S. Mota, A. L. Valverde, J. W. M. Carneiro and F. M. dos Santos Junior, *Org. Chem. Front.*, 2021, **8**, 2019; (e) M. O. Marcarino, S. Cicetti, M. M. Zanardi and A. M. Sarotti, *Nat. Prod. Rep.*, 2022, **39**, 58.
- For some recent examples of the use of empirical rules and chemical intuition alongside computational structure revisions, see: (a) A. G. Kutateladze, E. H. Krenske and C. M. Williams, *Angew. Chem., Int. Ed.*, 2019, **58**, 7107; (b) L. A. Maslovskaya, A. I. Savchenko, E. H. Krenske, S. Chow, T. Holt, V. A. Gordon, P. W. Reddell, C. J. Pierce, P. G. Parsons, G. M. Boyle, A. G. Kutateladze and C. M. Williams, *Chem. – Eur. J.*, 2020, **26**, 11862; (c) M. Elyashberg, I. M. Novitsky, R. W. Bates, A. G. Kutateladze and C. M. Williams, *Eur. J. Org. Chem.*, 2022, e202200572; (d) A. G. Kutateladze, R. W. Bates, M. Elyashberg and C. M. Williams, *Eur. J. Org. Chem.*, 2023, e202201316.
- (a) Y. Guan, S. V. S. Sowndarya, L. C. Gallegos, P. C. John and R. S. Paton, *Chem. Sci.*, 2021, **12**, 12012; (b) I. M. Novitskiy and A. G. Kutateladze, *Nat. Prod. Rep.*, 2022, **39**, 2003; (c) F. Hu, M. S. Chen, G. M. Rotskoff, M. W. Kanan and T. E. Markland, *ACS Cent. Sci.*, 2024, **10**, 2162; (d) F. Xu, W. Guo, F. Wang, L. Yao, H. Wang, F. Tang, Z. Gao, L. Zhang, E. Weinan, Z.-Q. Tian and J. Cheng, *Nat. Comput. Sci.*, 2025, **5**, 292.
- (a) E. Danelius, S. Halaby, W. A. van der Donk and T. Gonen, *Nat. Prod. Rep.*, 2021, **38**, 423; (b) L. J. Kim, M. Xue, X. Li, Z. Xu, E. Paulson, B. Mercado, H. M. Nelson and S. B. Herzon, *J. Am. Chem. Soc.*, 2021, **143**, 6578; (c) D. A. Delgadillo, J. E. Burch, L. J. Kim, L. S. de Moraes, K. Niwa, J. Williams, M. J. Tang, V. G. Lavallo, B. K. Chhetri, C. G. Jones, I. H. Rodriguez, J. A. Signore, L. Marquez, R. Bhanushali, S. Woo, J. Kubanek, C. Quave, Y. Tang and H. M. Nelson, *ACS Cent. Sci.*, 2024, **10**, 176.



- 70 A. W. Markwell-Heys and J. H. George, *Org. Biomol. Chem.*, 2016, **14**, 5546.
- 71 A. Grube, M. Assmann, E. Lichte, F. Sasse, J. R. Pawlik and M. Köck, *J. Nat. Prod.*, 2007, **70**, 504.
- 72 N. Iwata and S. Kitanaka, *J. Nat. Prod.*, 2010, **73**, 1203.
- 73 Y.-X. Yang, J.-X. Wang, Q. Wang, H.-L. Li, M. Tao, Q. Luo and H. Liu, *Fitoterapia*, 2018, **127**, 396.
- 74 L. Burchill, A. J. Day, O. Yahiaoui and J. H. George, *Org. Lett.*, 2021, **23**, 578.
- 75 L. Burchill and J. H. George, *J. Org. Chem.*, 2020, **85**, 2260.
- 76 F.-L. Chen, D.-L. Liu, J. Fu, J. Yang, L.-P. Bai, W. Zhang, Z.-H. Jiang and G.-Y. Zhu, *Chin. J. Chem.*, 2022, **40**, 460.
- 77 S. A. French, C. J. Sumby, D. M. Huang and J. H. George, *J. Am. Chem. Soc.*, 2022, **144**, 22844.
- 78 M. Resch, A. Steigel, Z.-L. Chen and R. Bauer, *J. Nat. Prod.*, 1998, **61**, 347.
- 79 S. Narayan, J. Muldoon, M. G. Finn, V. V. Folkin, H. C. Kolb and K. B. Sharpless, *Angew. Chem., Int. Ed.*, 2005, **44**, 3275.
- 80 M. A. Ischay, M. E. Anzovino, J. Du and T. P. Yoon, *J. Am. Chem. Soc.*, 2008, **130**, 12886.
- 81 H. Kinouchi, K. Sugimoto, Y. Yamaoka, H. Takikawa and K. Takasu, *J. Org. Chem.*, 2021, **86**, 12615.
- 82 (a) C. Chong, Q. Zhang, J. Ke, H. Zhang, X. Yang, B. Wang, W. Ding and Z. Lu, *Angew. Chem., Int. Ed.*, 2021, **60**, 13807; (b) J. Baars, I. Grimm, D. Blunk, J.-M. Neudorfl and H.-G. Schmalz, *Angew. Chem., Int. Ed.*, 2021, **60**, 14915; (c) L.-M. Deng, L.-J. Hu, W. Tang, J.-X. Liu, X.-J. Huang, Y.-Y. Li, Y.-L. Li, W.-C. Ye and Y. Wang, *Org. Chem. Front.*, 2021, **8**, 5728; (d) G. Schoenn, C. Kouklovsky, R. Guillot, T. Magauer and G. Vincent, *Angew. Chem., Int. Ed.*, 2025, e202505270.
- 83 (a) X.-W. Yang and R. B. Grossman, *Org. Lett.*, 2020, **22**, 760; (b) D. C. Holland and A. R. Carroll, *Molecules*, 2024, **29**, 594.
- 84 F.-C. Ren, L.-X. Wang, Y.-F. Lv, J.-M. Hu and J. Zhou, *J. Org. Chem.*, 2021, **86**, 10982.
- 85 (a) I. Cortes and A. M. Sarotti, *J. Org. Chem.*, 2023, **88**, 14156; (b) M. Elyashberg, S. Tyagarajan, M. Mandal and A. V. Buevich, *Molecules*, 2023, **28**, 3796.

